

# Impact of conventional and modified ring-spun yarn structures on the generation and release of fragmented fibers (microfibers) during abrasive wear and laundering

Textile Research Journal  
2023, Vol. 93(5–6) 1099–1112  
© The Author(s) 2022



Article reuse guidelines:

sagepub.com/journals-permissions  
DOI: 10.1177/00405175221127709  
journals.sagepub.com/home/trj



Abdul Jabbar<sup>1,2</sup>, Alma V Palacios-Marín<sup>1</sup> , Ali Ghanbarzadeh<sup>3</sup>,  
Dongmin Yang<sup>4</sup> and Muhammad Tausif<sup>1</sup> 

## Abstract

The abrasive wear of textiles during ordinary use and laundering results in fiber damage, which leads to the generation and release of fragmented fibers (FFs). Ring-spun yarn has a dominant share of about 70% of global spun yarn production. The effect of conventional and modified ring yarn structures (compact, SIRO and SIRO-compact) on FF release from cotton textiles during repeated abrasion and laundering was studied. All prepared cotton yarns and textiles are industrially and commercially relevant. The FFs formed during each abrasion and washing cycle were collected from textiles and quantified. The yarn tensile properties and fabric frictional characteristics were employed to explain the release of FFs. For the first time, the morphology of collected FF ends was associated with the fiber damage nature (granulated and fibrillated) induced by different types of stresses and experimental exposure conditions. The results demonstrated that modified ring yarn structures released a significantly lower FF mass as compared to conventional ring yarn structures. The tensile strength was decreased, and breaking elongation increased after repeated abrasion and washing. The fabric surface properties were also affected by abrasion and laundering. The yarn structure choices impact the amount of released FFs, which are dispersed into the environment as a pollutant or a carrier of pollutants with potential hazards to the health of the environment and living organisms.

## Keywords

Fragmented fibers, microfibers, microplastics, modified ring yarns, Martindale abrasion, fiber damage

The release of fragmented fibers (FFs), from both natural<sup>1,2</sup> and manufactured<sup>3–6</sup> textiles, is an established source of anthropogenic pollution in the aquatic and terrestrial environment. A fiber fragment is a short textile fiber (typically <5.0 mm long),<sup>7</sup> broken or separated away from a textile construction. The term ‘microfiber’ has also been commonly used to describe fibrous and/or microplastic pollution from textiles. Textiles are known to shed FFs during production,<sup>8</sup> everyday use,<sup>9</sup> laundering<sup>9–16</sup> and drying,<sup>17–19</sup> but also continue to release FFs after disposal.<sup>20</sup> In 2018, global fiber production reached 111 million tons<sup>21</sup> and is expected to grow at the rate of 3.7% per annum, reaching 130 million tons by 2025.<sup>22</sup> Among textile fibers, polyester and cotton are the dominant fibers used in the global production of textiles, with

approximate shares of 54.5% and 24.3% in global fiber production, respectively.<sup>21</sup> Polyester is a synthetic polymer fiber, whereas cotton is a natural cellulosic fiber. Rising clothing demand due to the increasing world population and fast fashion trends are the main reasons responsible for the increase in global

<sup>1</sup>School of Design, University of Leeds, UK

<sup>2</sup>Department of Textile Engineering, National Textile University, Pakistan

<sup>3</sup>School of Mechanical Engineering, University of Leeds, UK

<sup>4</sup>School of Engineering, University of Edinburgh, UK

## Corresponding author:

Dr Muhammad Tausif, School of Design, University of Leeds, Leeds, LS2 9JT, UK.

Email: m.tausif@leeds.ac.uk

fiber production and textile consumption,<sup>23</sup> which ultimately leads to a rise in anthropogenic pollution.

Several studies have reported polyester textiles as a dominant source of anthropogenic pollution.<sup>10,13,24-27</sup> However, the presence of both natural and synthetic fibers in the environment has been reported. Despite some studies having shown cotton fibers to be biodegradable in fresh water and the marine environment,<sup>28,29</sup> there are still some concerns in the published literature about the fate and role of natural fibers in the aquatic environment.<sup>3,30,31</sup> For example, the presence of colorants and other chemical additives in cotton textiles modifies the chemical nature of natural cellulose, which may complicate the biodegradation process and aquatic toxicity of these microfibers in the marine environment.<sup>32</sup> A recent study discloses that cotton fabrics dyed with reactive dye or treated with a water repellent finish are less biodegradable in seawater than untreated cotton specimens.<sup>33</sup> Athey et al.<sup>1</sup> identified the presence of modified cellulose microfibers, originating from indigo dyed cotton denim jeans, in aquatic environments serving as a tangible and potent indicator of anthropogenic pollution.

Staple spun yarns account for some 45% of global yarn production,<sup>34</sup> with cotton being a leading fiber consumed in the spun yarn industry.<sup>35</sup> Ring spinning is the dominant technology (despite being nearly 200 years old) in the spun yarn industry, with a share of about 70% of global spun yarn production technologies<sup>36</sup> due to the better suitability of the ring-spun yarn structure and properties to a wide range of textile applications.<sup>37</sup> Since the invention of ring spinning, it has gone through many developments to increase the productivity of conventional systems and improve the quality of ring-spun yarn. Among different advancements, modified ring spinning systems (especially compact, SIRO and SIRO-compact) have brought substantial modifications to the conventional ring spinning process with the aim of changing the structural arrangement of fibers in the yarn.<sup>38</sup> The better structural integrity of fibers in the yarn may result in improved fiber cohesion within the yarn structure,

which may contribute to less fabric wear during ordinary everyday use and laundering, and hence less release of FFs during the whole service life of the textiles. A schematic representation of differences in the yarn formation principle of the mentioned ring-spun yarns is shown in Figure 1. Briefly, the main difference in conventional and modified ring spinning systems is in the geometry of the yarn formation zone, that is, the spinning triangle, which results in a different structural arrangement of fibers in the yarn. Conventional ring spinning has a normal spinning triangle whose width depends on the width of the drafted fiber strand and spinning tension during yarn formation. In compact spinning, the width of the spinning triangle is significantly reduced due to condensing of fiber strands before yarn formation. In SIRO spinning, the main spinning triangle is divided into two primaries and one final spinning triangle by feeding two rovings in parallel at a predetermined spacing through the drafting unit. In SIRO-compact spinning, both the compact and SIRO spinning principles are combined.

Textiles wear out and release FFs mainly due to abrasive wear and breakage of textile fibers during manufacturing, use and laundering.<sup>32</sup> In textiles, the wear of fibers, yarns and fabrics is caused by a rubbing action that involves relative motion between two fabric surfaces or a fabric surface and another material.<sup>39</sup> There are different parameters that influence the generation and release of FFs from textiles, including the physicochemical properties of textile fibers and their morphology, yarn type and structure, fabric type and geometry and textile processing history.<sup>32</sup> De Falco et al.<sup>9</sup> disclosed the lowest release of FFs from textiles with a very compact woven structure and highly twisted yarns made of continuous filaments compared to that of an open structure. Raja Balasaraswathi and Rathinamoorthy<sup>40</sup> studied the effect of the knitted fabric structure and fabric mass areal density on FF shedding from 100% polyester textiles. It was reported that interlock knitted structures shed more FFs during laundry compared to 1×1 rib and single jersey

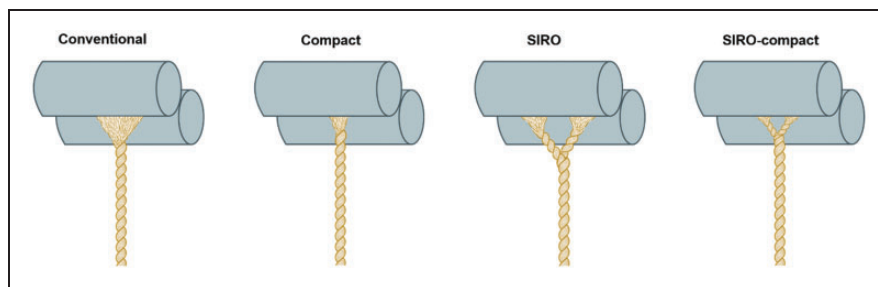


**Figure 1.** Schematic representation of yarn formation principles during ring spinning (dimensions not to scale).

structures. Furthermore, fabric structural parameters, such as higher stitch density, higher tightness factor, lower loop length and less fabric mass areal density, resulted in reduced FF shedding. A recent study elucidated the impact of key yarn structures and material composition on the number of released FFs and the fiber length distribution profile.<sup>41</sup> Similarly, another study reported the influence of fabric geometrical parameters on FF release.<sup>42</sup>

In a correlation study to compare the actual fabric wear with laboratory abrasion and laundering, laboratory abrasion followed by laundering reproduced very similar results to the actual wear of fabric during ordinary use compared to laboratory abrasion or laundering alone.<sup>43</sup> Therefore, the objective of the present study is to understand the influence of ring spinning variants (conventional, compact, SIRO and SIRO-compact) on the release of FFs from textile fabrics by simulating fabric wear during ordinary use with laboratory abrasion followed by laundering processes. For the first time, released FF end morphology was studied and associated with the number of exposure cycles. The outcome of this study will not only help to give an insight into the effect of the structural arrangement of fibers in the yarn on the release of FFs from textiles, but also provide insights on yarn structural choices to mitigate the generation of FFs released during wearing and laundering. This can help to at-source decrease the release of FFs in both dry and wet environments, compared to end-of-pipe approaches to capture the released FFs, which are mainly designed for released FFs during laundering.

**Table 1.** Properties of Pima cotton fibers used in the study

Sr. no.	Parameters	Values
1	Upper half mean length (mm)	37.008 ± 0.686
2	Fineness (micronaire)	4.58 ± 0.05
3	Tenacity (g <sub>f</sub> /tex)	43.5 ± 0.6
4	Breaking elongation (%)	6.9 ± 0.6
5	Uniformity index (-)	87.8 ± 1.0
6	Short fiber index (%)	4.0 ± 0.1
7	Degree of yellowness, +b (-)	13.7 ± 0.2
8	Degree of reflectance, +Rd (-)	69.6 ± 0.6

**Table 2.** Properties of ring-spun yarns

Sr. no.	Ring-spun yarn	Actual count (tex)	Unevenness (%)	Total imperfections/km	Hairiness index (-)	Tenacity (cN/tex)	Breaking elongation (%)
1	Conventional	14.41 ± 0.07	11.84 ± 0.33	261 ± 42	5.45 ± 0.12	19.14 ± 1.56	4.93 ± 0.38
2	Compact	14.89 ± 0.11	11.29 ± 0.18	231 ± 33	5.07 ± 0.04	21.98 ± 2.48	5.41 ± 0.53
3	SIRO	15.21 ± 0.03	11.73 ± 0.70	286 ± 62	4.68 ± 0.14	21.78 ± 1.84	5.70 ± 0.46
4	SIRO-compact	15.53 ± 0.07	12.54 ± 0.29	573 ± 61	4.33 ± 0.07	23.49 ± 1.78	5.90 ± 0.34

## Materials and methods

### Yarn and fabric preparation

Four types of carded ring-spun yarns, namely conventional, compact, SIRO and SIRO-compact, were produced using Pima cotton, as listed in Table 1. The raw cotton fibers were processed through a blow room line (Toyoda-Ohara-Hergeth), carding machine (Howa CM80), breaker drawing frame (Toyoda DYH 500C), finisher drawing frame (RSB D40), roving frame (Toyota FL-16) and ring frame (Toyota RY-5 for normal and SIRO yarns and Rieter K-44 for compact and SIRO-compact yarns) to produce carded ring-spun yarns of linear density 14.76 tex (40.0 Ne) with a nominal twist level of 10.71 turns.cm<sup>-1</sup> (27.20 turns.inch<sup>-1</sup>) in all samples. The properties of the produced yarns are given in Table 2. The yarns were converted into a plain-woven fabric with thread densities of 35.43 threads cm<sup>-1</sup> (90 threads inch<sup>-1</sup>) in the warp direction and 29.92 threads cm<sup>-1</sup> (76 threads inch<sup>-1</sup>) in the weft direction on a sample rapier-weaving loom by CCI Tech Incorporated, Taiwan. The warp yarns were treated (sized) with polyvinyl alcohol (PVA) solution before weaving to reduce thread breakages during the weaving process. The fabric samples were named conventional, compact, SIRO and SIRO-compact, based on the yarn.

### Fabric pre-treatment and dyeing

The fabric samples were washed with 1.0 g.l<sup>-1</sup> Invadine® PBN at 80°C for 45 min, maintaining a liquor ratio of 10:1, and scoured and bleached in a single step using 1.5% w/w NaOH and 5.0% v/w H<sub>2</sub>O<sub>2</sub> at 80°C for 90 min with a liquor ratio of 5:1 followed by rinsing, neutralization and drying at room temperature for 24 h. To identify any cross-contamination, the bleached fabrics were dyed into four different colors by the exhaust method using Remazol Red 3B for conventional fabric, Remazol Golden Yellow RGB for compact fabric, Remazol Brilliant Blue BB for SIRO fabric and Remazol Black B for SIRO-compact fabric. The dyeing process was carried out at 1% owf of each dye in 80 g.l<sup>-1</sup> NaCl

and  $20 \text{ g.l}^{-1} \text{ Na}_2\text{CO}_3$  at  $60^\circ\text{C}$  with a liquor ratio of 20:1 according to the dyeing procedure presented in Figure 2. The fabrics were washed with  $0.5 \text{ g.l}^{-1}$  Invadine® PBN at  $100^\circ\text{C}$  for 30 min and then rinsed thoroughly with tap water, neutralized and dried again at room temperature.

### Sample preparation for Martindale abrasion

This study aimed to simulate fabric wear during ordinary use by employing multiple cycles of rubbing and subsequent laundering to understand the influence of four different ring-spun yarn structures on the release of FFs from textiles. The fabric-to-fabric rubbing was carried out on a Martindale abrasion tester (James Heal 5-station Martindale abrasion tester, model 1305). The fabric samples were cut into square sizes of  $6.5 \times 6.5 \text{ cm}^2$  (specimen) and  $16 \times 16 \text{ cm}^2$  (abradant) from the same fabric sample. Using Coats Astra (Tkt 120, 13ANT) 27 tex 100% staple spun polyester thread of light green color, the samples were overlocked, folded 0.5 cm from each side and sewn using the same thread. The overlocking/sewing thread color was intentionally different from colors of the textile samples to differentiate any release of FFs from the sewing thread.<sup>41</sup> The final sizes of the specimen and abradant were  $5.5 \times 5.5 \text{ cm}^2$  and  $15 \times 15 \text{ cm}^2$ , respectively. Textile manufacturing processes involve fiber–fiber, fiber–metal and fiber–water interactions, which are known to cause fiber damage, leading to a higher amount of FF generation in the first cycle.<sup>41</sup> Hence, all samples were subjected to a prewashing step, without using any steel balls, to collect FFs associated with textile manufacturing and to remove any contaminants, excess dye, dust and dirt particles. The prewashing was carried out at  $40^\circ\text{C}$  for 45 min at 40 rpm in standardized laboratory laundry equipment (GyroWash, James Heal) using 100 and 250 ml of distilled water for the specimen and abradant, respectively. The steel canisters were thoroughly washed with

distilled water before the washing operation. Some 2.7% omf of American Association of Textile Chemists and Colorists (AATCC) high-efficiency standard reference liquid detergent without optical brightener was added in distilled water for prewashing of the samples. After prewashing, the samples were rinsed with distilled water thoroughly and dried in an oven at  $50^\circ\text{C}$  overnight.

### Martindale abrasion and collection of FFs

As per ISO-12974:2, a preliminary abrasion test was conducted, and the abrasion resistance was found to be 3500–4000 rubs for the fabrics under study. Since the current study is aimed to simulate the actual fabric wear during ordinary use, repeated laboratory abrasion followed by laundering cycles was employed to understand the influence of the selected ring yarn structures on the release of FFs from textiles. The specimen was abraded to 500 rubs against the abradant by applying 12 kPa pressure. The abrasion experiment was stopped after 500 rubs, and both the specimen and abradant were separately subjected to washing. This abrasion and laundering cycle was repeated six times, and FFs were collected during each cycle separately from the specimen and the abradant. The ISO-12974:2 standard was modified as per Cai et al.<sup>27</sup> to avoid cross-contamination of the collected FFs, and the modified experimental setup is shown in Figure 3. As a substitute to underlay polyurethane foam and woven felt, rubber sheets of 1.0 mm thickness were used. Furthermore, the same test textile as the specimen was replaced with a standard abradant (woven wool fabric) to simulate the same fabric-on-fabric abrasion. It was recognized by Cai et al.<sup>27</sup> that mounting a cylinder on each abrasion station does not allow the escape of FFs generated

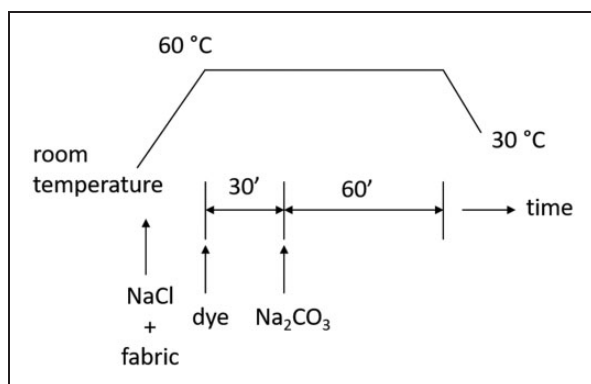


Figure 2. Textile dyeing procedure.

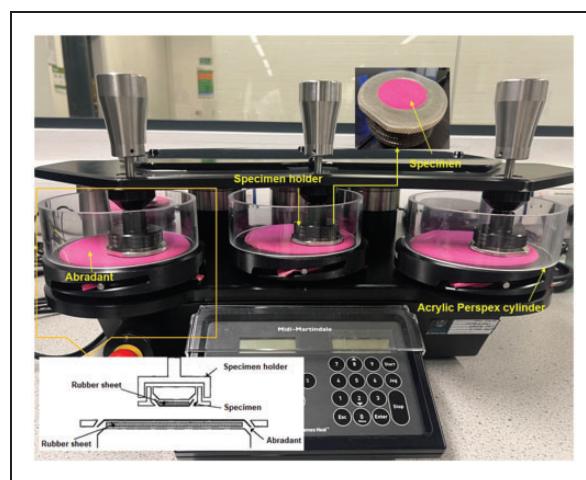


Figure 3. The Martindale abrasion with a modified experimental setup.

during the abrasion experiment, so an acrylic Perspex cylinder, having height of 50 mm, inner diameter of 140 mm and thickness of 5 mm, was mounted around each of the test stations to collect the generated FFs and to avoid cross-contamination between samples during the abrasion test.

After each cycle (abrasion and laundering), the apparatus parts (Perspex ring, rubber underlay and metallic sample holders) exposed to the specimen and abrasant were rinsed three times using distilled water separately, and the effluent was recovered for subsequent filtration. The FFs were collected from textile samples (specimen and abrasant) separately by employing the same laundering procedure outlined in the *Sample preparation for Martindale abrasion* section. Post laundering, the effluent was collected in a beaker. A pair of tweezers was used to remove excess water from the textile samples, and the detergent foam was removed by rinsing the specimen in distilled water. The open mesh, beakers and tweezers were rinsed three times. All recovered effluent from apparatus parts, laundering and rinsing the textile samples was then collected in one beaker for subsequent filtration. The laundered samples were left to dry in a fan oven for a minimum of 4 h at 50°C and then conditioned again for the next abrasion and laundering cycle. The beaker and glass funnel were also rinsed three times, and all the collected effluent was filtered using a binder-free glass fiber filter of 1.6 µm mean pore size and 47 mm diameter (Merck Millipore Ltd, Ireland). The filters were weighed before filtration using a precision balance (Mettler Toledo AE160, resolution of 0.00001 g). After filtration, the filters were placed in a fan oven overnight at 50°C, conditioned for 4 h and re-weighed to determine the increase in filter mass, which corresponds to the amount of released FF from textile samples. The order of experiments was randomized to minimize the chances of systematic error. During the experiments, protective nitrile gloves and a white laboratory coat were worn to minimize any cross-contamination.

### Testing and characterization

The yarns were carefully taken out from the warp direction of the abrasant fabric before the start and after the sixth cycle to quantify any change in the tensile properties of yarns during repeated abrasion and laundering. Following this, 20 yarn specimens from each fabric sample were tested on a universal testing machine at 100 mm gauge length and with a 5 kN load cell (Titan, James Heal). The surface roughness and coefficient of friction of the abrasant in the warp direction ( $n=4$ ), before the start and after the sixth cycle, were measured using a Kawabata KES-FB4 surface

tester to record any changes in surface properties during repeated abrasion and laundering. The fiber ends of FFs collected on glass filters after the first and sixth abrasion and laundering cycles for conventional and SIRO-compact fabric samples were analyzed using a scanning electron microscope (SEM; Jeol JSM-6610, Japan) to characterize the types of fiber damage during abrasion and washing. Three filters from each sample were randomly selected and analyzed to get three or four images of damaged fiber ends from each filter to get a total of 10 SEM images. The filters were sputter-coated with a 60 µm gold layer by using a sputter coater (Q150RS by Quorum Technologies). Tukey's comparison method, using one-way analysis of variance (ANOVA), was employed to compare the statistical significance of the release of FF mass from the four different fabrics during repeated abrasion and laundering cycles. Student's *t*-test was used to determine the statistical significance of the results of the yarn tensile properties and Kawabata surface properties before the start and after the sixth abrasion and laundering cycle.

## Results and discussion

### *The release of FF mass during repeated abrasion and laundering*

The mass of FFs collected from the abraded specimens and abrasants after each of the six abrasion and laundering cycles for each fabric sample is plotted in Figure 4. It is evident that the specimen of the conventional sample releases a higher amount of FFs compared to the rest of the samples. This is supported by statistical analysis (Table 3), which shows a significant difference in collected FF mass from the conventional specimen compared to the remaining three structures for up to the fifth cycle. The fibers undergo fiber-to-fiber and fiber-to-metal friction during textile manufacturing, leading to fiber fatigue or fracture.<sup>44</sup> The higher release of FFs during the first cycle can be associated with the accumulated effect of abrasion and fiber damage during textile manufacturing. For the specimen (Figure 4), this release of FF mass decreases gradually up to the third cycle, and generally there is steady-state behavior in the subsequent cycles for each textile sample.

For the abrasant fabric (Figure 4), generally, there is a consistent release of FF mass in all cycles. This is evident by the statistical analysis (Table 3), which shows a significant difference in collected FF mass by the conventional abrasant compared to the remaining three structures only during the first cycle. The specimens release a higher amount of FF as compared to the abrasants for all textile samples after each abrasion

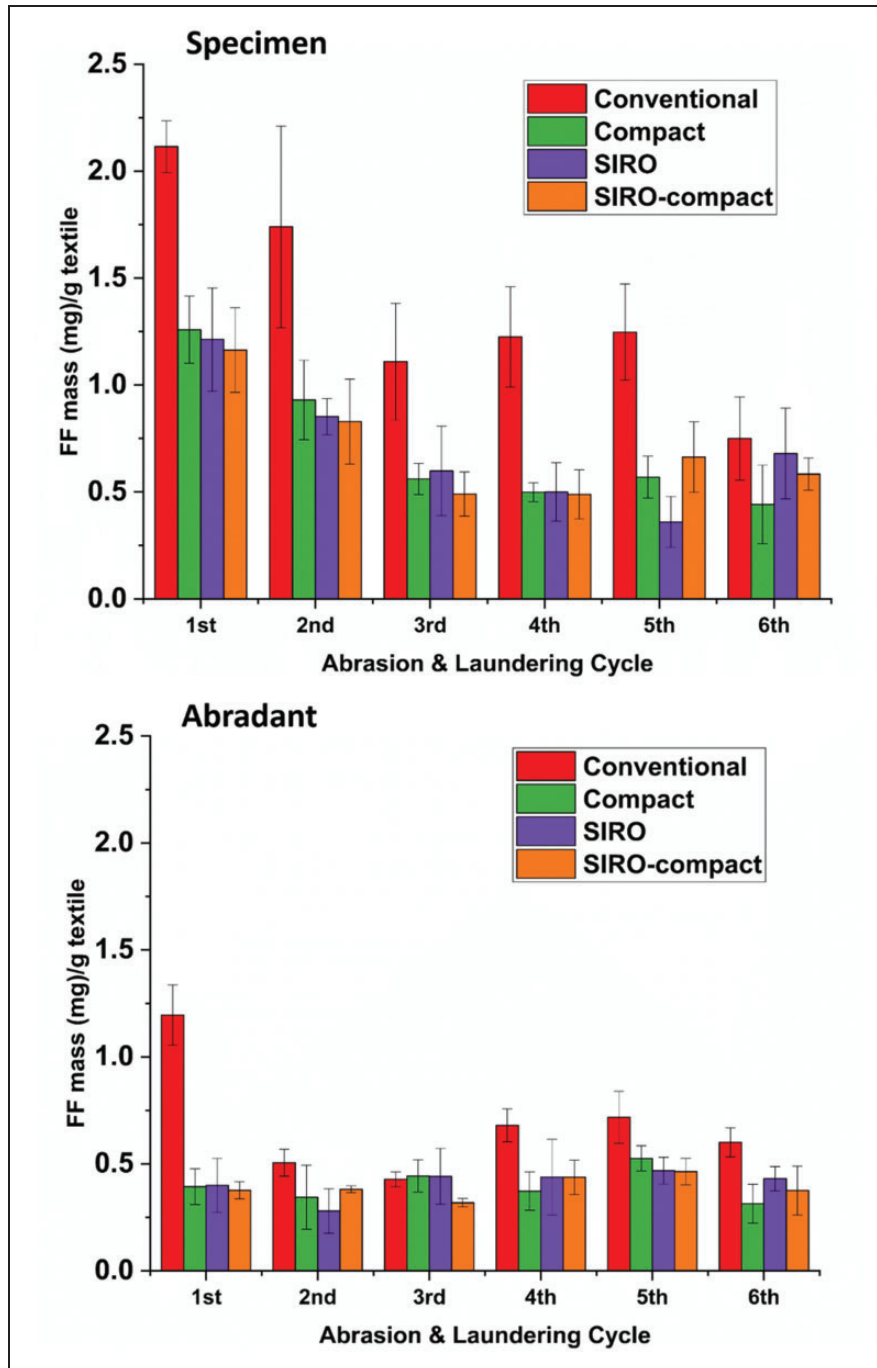


**Figure 4.** Fragmented fiber (FF) mass collected from wash effluent after abrasion and laundering of the abraded specimens and abradants.

and laundering cycle, as shown in Figure 4. During the Martindale abrasion process, the exposed area of the specimen is continuously rubbed against the abradant, so the fibers in the exposed area of the specimen are under continuous tensile and/or shear stresses, leading to more fiber damage and the generation of FFs, irrespective of the type of fiber and the yarn/fabric structure, whereas the fibers in the exposed area of the

abradant are intermittently rubbed due to the Lissajous pattern of rubbing (as recommended in standard ISO-12974:2) during Martindale abrasion, and hence less fiber damage and generation of FFs.

The results demonstrate that textiles produced from the conventional yarn shed more FFs compared to textiles produced from compact, SIRO and SIRO-compact yarns. The yarn structure (i.e., the geometrical

**Table 3.** Significance values by Tukey's statistical analysis for comparison of fragmented fiber (FF) mass release of the normal sample with compact, SIRO and SIRO-compact fabrics

Variable	By	Abrasion and laundering cycles					
		1	2	3	4	5	6
<i>Specimen</i>							
Conventional (FF mass, mg/g)	Compact (FF mass, mg/g)	0.001*	0.017*	0.024*	0.000*	0.001*	0.192
	SIRO (FF mass, mg/g)	0.000*	0.009*	0.036*	0.000*	0.000*	0.960
	SIRO-compact (FF mass, mg/g)	0.000*	0.008*	0.011*	0.000*	0.004*	0.660
<i>Abradant</i>							
Conventional (FF mass, mg/g)	Compact (FF mass, mg/g)	0.000*	0.228	0.904	0.028*	0.053	0.002*
	SIRO (FF mass, mg/g)	0.000*	0.061	0.959	0.093	0.012*	0.053
	SIRO-compact (FF mass, mg/g)	0.000*	0.434	0.289	0.092	0.010*	0.138

\*Statistically significant at the 95% confidence level.

arrangement and binding of fibers in the yarn) may likely to be an important characteristic, among other factors, affecting the generation and release of FFs from textiles. The yarn structure largely depends on fiber migration, and the geometrical arrangement of fibers in staple spun yarns.<sup>45</sup> Fiber migration, which is described as the relative movement of a fiber with respect to its neighboring fibers during yarn formation and its ultimate position in the yarn body,<sup>46</sup> affects the compactness (packing fraction) and binding of fibers in the yarn. In the current study, all textile samples were made from ring-spun yarns that were produced by conventional and modified ring spinning systems. The modified ring spinning systems, including compact, SIRO and SIRO-compact, alter the flow behavior of fibers in the yarn formation zone and/or the geometry of the spinning triangle at the exit of the drafting system, which leads to a decisive impact on the yarn structure and properties, including higher fiber migration,<sup>47</sup> compactness and tenacity and less hairiness<sup>48</sup> as compared to conventional ring spinning. The higher fiber migration and compactness would lead to an increase in inter-fiber friction and cohesive forces holding the fibers together in the yarn. Therefore, the deformation developed in fibers due to induced mechanical stresses during downstream textile production processes and abrasive wear may dissipate largely to neighboring fibers in the yarn body, resulting in comparatively less damage, removal or displacement of fibers and ultimately less generation of FFs.

### Tensile properties of yarns

The results of the tensile strength and breaking extension of yarns, removed from the warp direction of the abradant samples, before the start and after the sixth cycle, are plotted in Figures 5(a) and (b), respectively. The tensile strength of yarns decreased, while the breaking extension increased for all samples.

However, the differences were only significant for conventional and compact yarns (Table 4). SIRO and SIRO-compact yarn structures offer higher fiber migration and entanglement of fibers during yarn formation. For example, Soltani and Johari<sup>47</sup> observed that SIRO spun yarns demonstrate higher migration parameters as compared to compact and conventional ring-spun yarns at similar twist levels. The higher fiber migration leads to a coherent self-interlocking yarn structure in which the fiber movement or slippage is restricted.<sup>49</sup> Hence, the improved yarn structure coupled with significantly less generation of FFs during abrasion (Figure 4) may contribute to better retention of tensile strength after repeated abrasion and laundering. The increase in breaking extension is statistically significant for all samples (Table 4). There might be a release of residual stresses among fibers in the yarn upon successive abrasion and laundering, causing the yarn structure to relax and extend more before breaking. Furthermore, during tensile loading, the applied load is distributed among the fibers in the yarn. The yarns in the fabric may become weaker during repeated abrasion and laundering, possibly due to fiber fatigue and fiber damage. Subject to repeated abrasion and laundering, the yarn microstructure is likely to be affected, leading to a change in inter-fiber cohesion and inter-fiber friction. The change in microstructure compounded with fiber damage may lead to the decrease in strength of the yarns and an increase in extension at break.

### Evaluation of the surface friction coefficient and roughness

The measured values of the KES coefficient of friction (MIU) and surface roughness (SMD) in the warp direction of the abradant samples before the start and after the sixth cycle are shown in Figures 6(a) and (b), respectively. The frictional coefficient is increased for

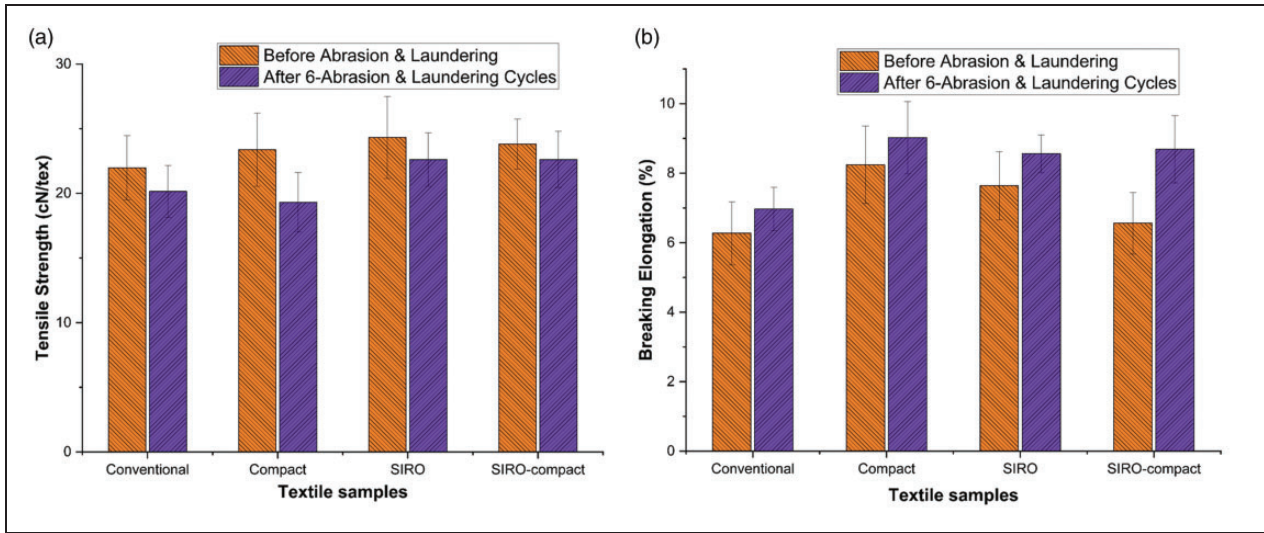


Figure 5. (a) Tensile strength and (b) breaking elongation of yarns before the first and after the sixth cycle of abrasion and laundering.

Table 4. Significance values from Student’s t-test for statistical significance of the tensile properties of the yarns and surface properties of textile samples before and after the abrasion and laundering cycles

Variable	Tensile properties of yarns		Kawabata fabric surface properties	
	Tensile strength (cN/tex)	Elongation (%)	MIU (–)	SMD (µm)
Conventional	0.018*	0.009*	0.009*	0.058
Compact	0.000*	0.032*	0.001*	0.341
SIRO	0.057	0.001*	0.033*	0.304
SIRO-compact	0.786	0.000*	0.008*	0.401

\*Statistically significant at the 95% confidence level.

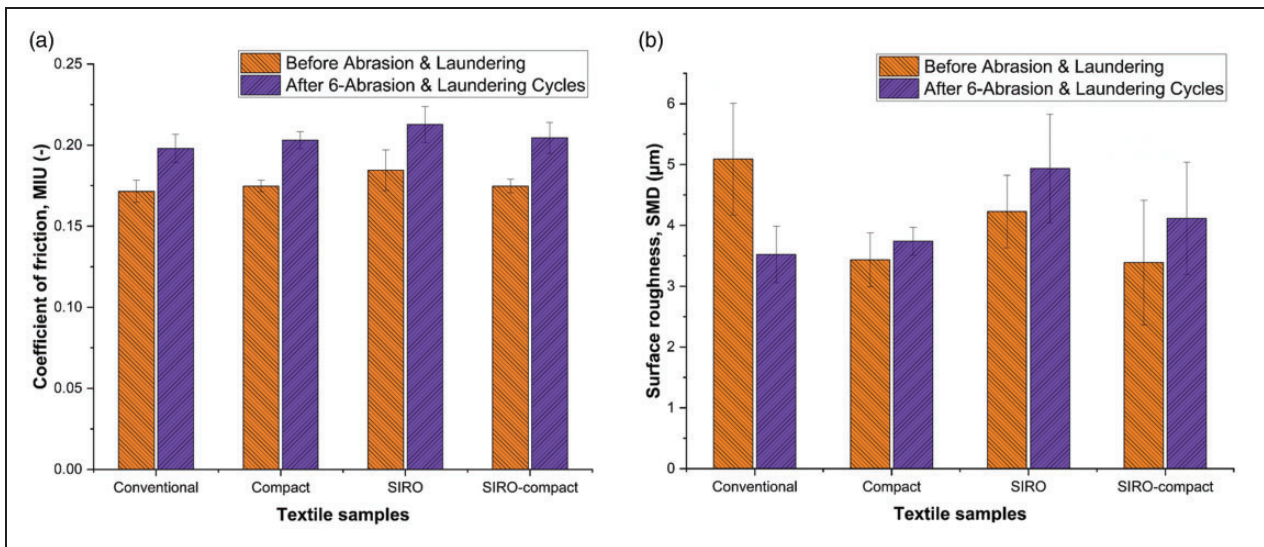


Figure 6. (a) Coefficient of surface friction and (b) surface roughness of the abrasants before the first and after the sixth cycle of abrasion and laundering.

all textile samples, and the increase is statistically significant, as shown by the statistical significance values in Table 4. The coefficient of friction is a function of a number of parameters, such as the material properties, normal force, contact geometries and environmental factors.<sup>50</sup> Since the normal force is constant during the abrasion experiment, the increase in the coefficient of friction after the sixth cycle may be explained by the increase in the surface area in contact. At zero cycles, the contact area between the specimen and abradant is assumed to be small. However, after repeated abrasion and laundering, FFs generated due to frictional wear are extracted and the contact area is supposed to be increased, which may be attributed to the increase in the coefficient of friction of the textile samples (Figure 6(a)).

The surface roughness depicts a decrease for the conventional sample but increase for the compact, SIRO and SIRO-compact samples, as shown in Figure 6(b). Nevertheless, all changes in surface roughness are statistically insignificant (Table 4). Furthermore, the average coefficient of variation of roughness was high, with values of 13.03% and 10.66% for the zero cycle and after the sixth cycle, respectively. This suggests that the conventional sample is the roughest at zero cycles, possibly due to poor fiber alignment, higher yarn hairiness and a higher percentage of folded and entangled fibers in the yarn body.<sup>49</sup> In comparison, the compact, SIRO, and SIRO-compact yarns have better fiber orientation

and binding of fibers in the yarn body and low hairiness as compared to the normal sample, which can be associated with a low surface roughness of the corresponding textile samples at zero cycles. During frictional wear dominated by an adhesion mechanism, the decrease in surface roughness will result in increased frictional force in contact.<sup>51</sup> The continuous higher release of FFs from the conventional sample may be associated with a decrease in amplitude of variation in the surface, resulting in a decrease in surface roughness after the sixth cycle. The surface appearance of the conventional sample after the sixth cycle is visible in Figure 7(a), which shows noticeable surface abrasion with fiber fuzziness. However, more coherent modified ring yarn structures, with relatively less release of FFs than that of the conventional sample, may offer more resistance to a decrease in amplitude of variation in the fabric surface. For the compact, SIRO and SIRO-compact samples, the presence of some pilling, as shown in Figures 7(b)–(d) respectively, may also be due to the increased amplitude of variation in the surface, causing an increase in surface roughness.

#### *Scanning electron microscopy for the morphological analysis of fragmented fiber ends*

The morphology of fiber ends can be associated with the nature of fiber damage induced by different types of stresses and exposure conditions.<sup>52</sup> Hence, the microscopic examination of damaged fiber ends in the FF

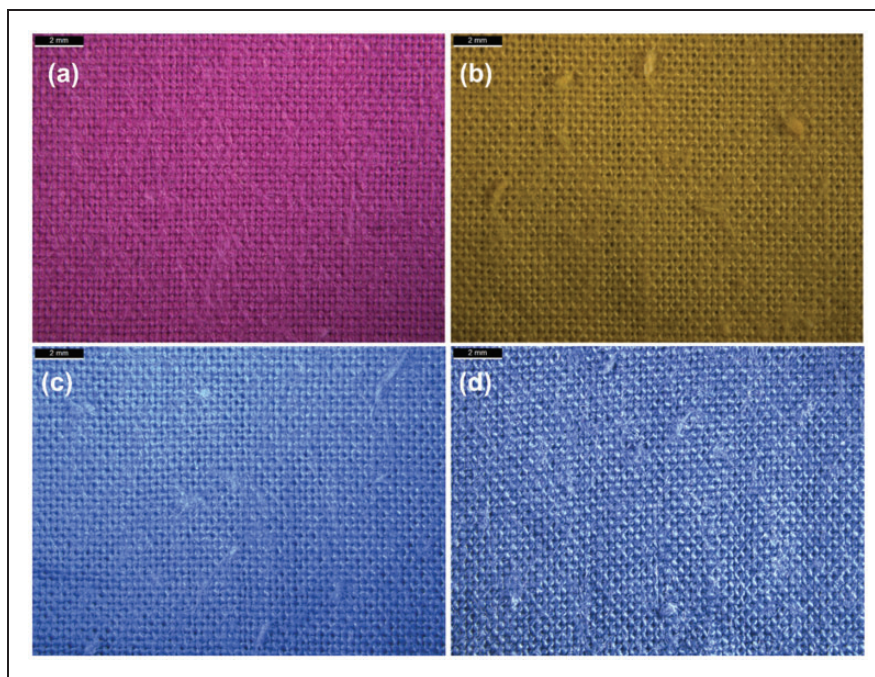


**Figure 7.** Light microscopic images of (a) normal, (b) compact, (c) SIRO and (d) SIRO-compact textiles samples after the sixth abrasion and laundering cycle.

mass was carried out to understand the nature of the failure mechanism of fibers in reference to different yarn structures. SEM examination of the collected FFs (over a glass fiber filter) of the conventional and SIRO-compact abrasant samples after the first and sixth cycles of abrasion and laundering was performed and is presented in Figures 8 and 9, respectively. Ten fiber ends were randomly imaged from the surface of each glass filter of the conventional and SIRO-compact samples. The granulated/transverse damage with a short length of independent fibril separation (Figures 8(a-1), 8(b-1), 9(a-1) and 9(b-1)) and fibrillated damage/longitudinal splits (Figures 8(a-2), 8(b-2), 9(a-2) and 9(b-2)) were found to be the main types of fiber damage. Previous studies suggest that FFs/microfibers may already be contained in textiles, which could originate from the textile production processes.<sup>10,53</sup> These FFs are found to be present in various textile products before the start of their use phase. The transverse damage ends of FFs prominent after the first cycle,

as shown in Figures 8(a-1) and 9(a-1), may suggest the history of mechanical stresses and high energy cuts induced during textile production processes, which are likely to be released from textiles due to their mobilization from the textile structure during the first abrasion and laundering cycle. This may further suggest that the majority of the transverse damaged FFs are less likely to be formed during the abrasion process but are only released from the yarn (textile) structure during the first exposure cycle.<sup>27</sup> Despite the prewashing of the textile samples done in the present study to remove already existing FFs in the textile structures, no further steps were undertaken to ensure the removal of textile production associated with FFs before starting the abrasion and laundering cycles. Therefore, further understanding of the prewashing (such as additional prewashing steps) is necessary to ensure that all pre-existing FFs have been removed. This, aided with the study of the nature of fiber damage by microscopic examination of the

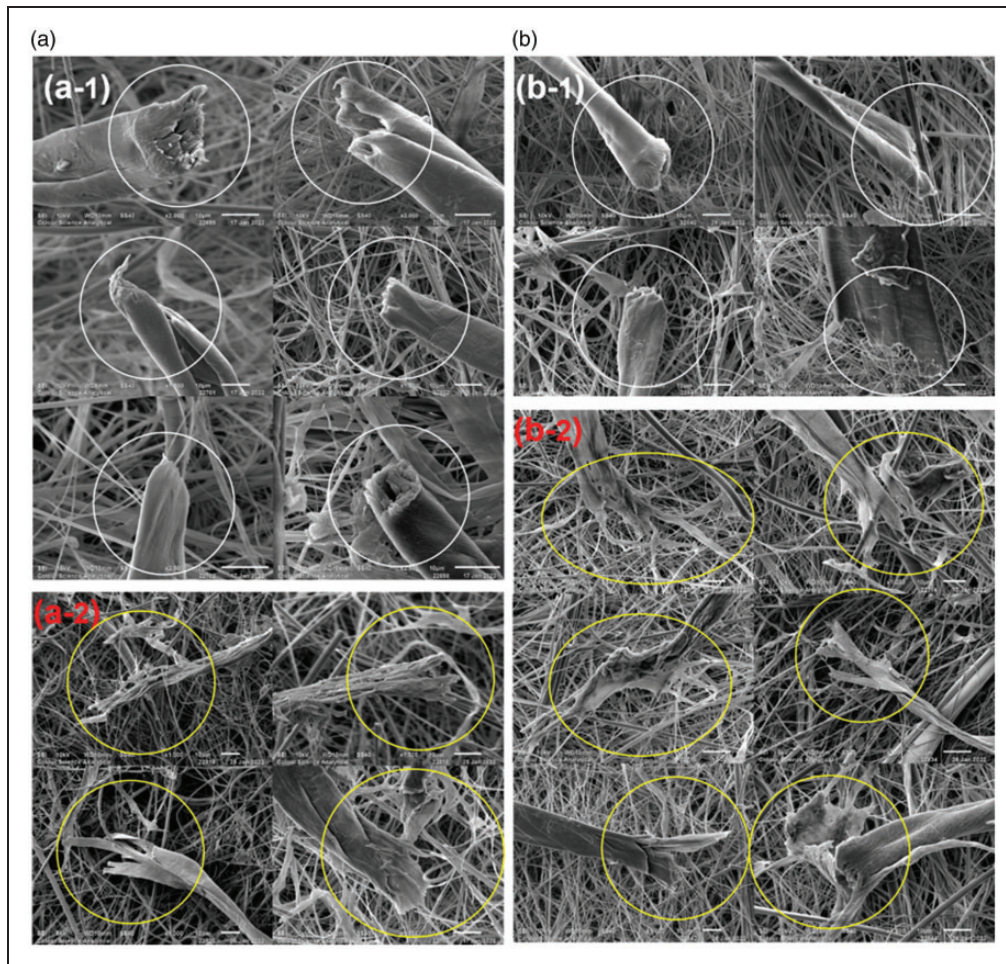


**Figure 8.** Characterization of fractured fiber ends released from the conventional sample after (a) the first cycle and (b) the sixth cycle of abrasion and laundering.

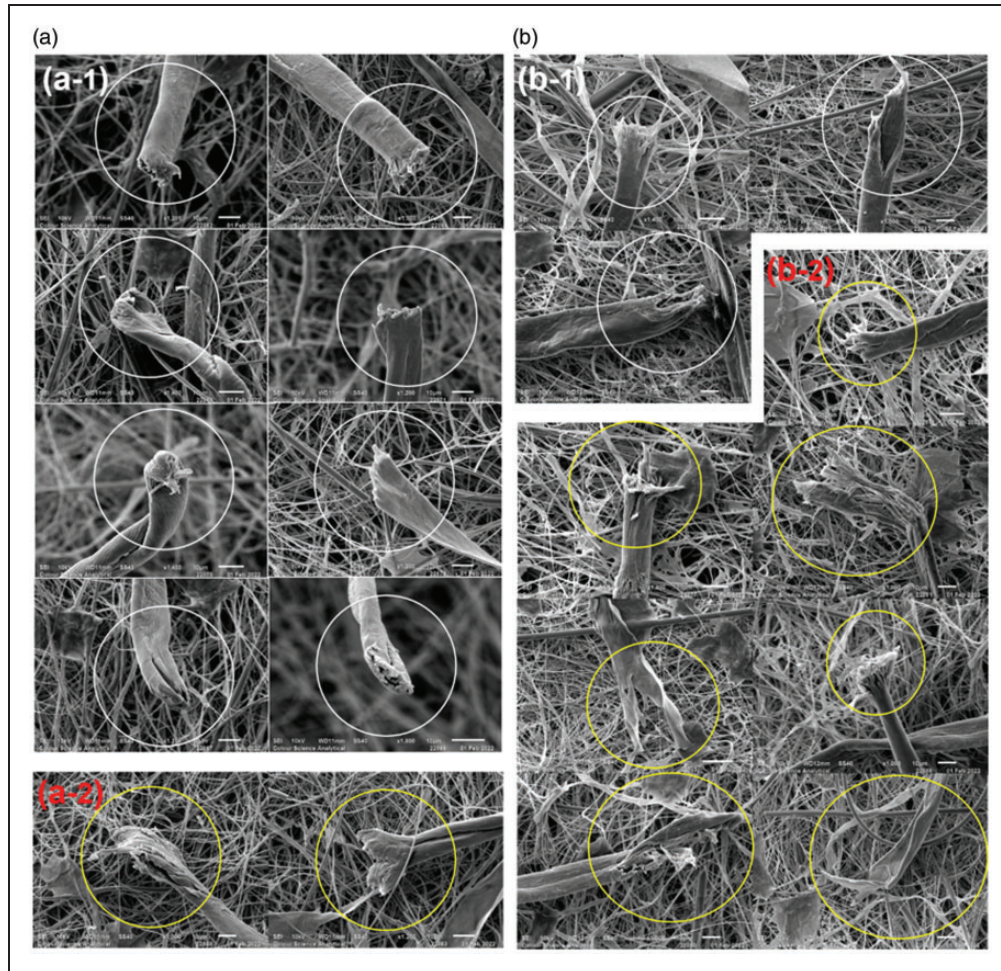


**Figure 9.** Characterization of fractured fiber ends released from the SIRO-compact sample after (a) the first cycle and (b) the sixth cycle of abrasion and laundering.

damaged fiber ends, would help to differentiate between the FFs originating from manufacturing or from the exposure cycles.

The magnitude of frictional force between the specimen and abradant during the abrasion experiment may be an additional possible influencing factor affecting the type of fiber damage. The Kawabata surface evaluation of the abradant, as shown in Figure 6, highlights that the coefficient of friction is less at the initial cycles for all samples, and increases after the sixth cycle. This indicates that the frictional wear of textiles samples is dominated by adhesion.<sup>51,54</sup> At the start of abrasion and laundering experiments, contact may occur at the tips of asperities due to surface roughness, and the applied load may be distributed in a small real contact area, which may be responsible for rupturing the fibers due to a greater deformation by the development of tensile and shear stresses, leading to transverse damage during abrasion. However, in the remit of this study, it was not possible to differentiate between

transversely damaged FFs from the abrasion process and those from textile manufacturing.

The abrasion process leads to fiber fatigue, rupture and fibrillation, which may induce fibrillated damage after the first cycle (Figures 8(a-2) and 9(a-2)). A relatively strong adhesion between two fabric surfaces, likely due to an increase in the contact area after successive abrasion and laundering, may result in shear failure of the fibers under repeated flexing and rotational fatigue, leading to the more yielding and plastic deformation, which may be responsible for interfibrillar slippage and noticeable fibrillated fiber damage,<sup>55</sup> with more scattering and progressive cracking paths generally observed after the sixth cycle (Figures 8(b-2) and 9(b-2)). Moreover, repeated deflection of surface fibers under the influence of periodic mechanical stresses during rubbing cycles may add to strong fibrillation after repeated abrasion and laundering with the rupture of fibers into fine fibrils, as shown in Figures 8(b-2) and 9(b-2). The fibers at or near the fabric surface

bear the highest stresses, and repeated and periodic rubbing deform the surface fibers, leading them to fibrillate and ultimately rupture. The fibrils under stress are much finer and therefore less resilient in response to mechanical stresses compared to the non-fibrillated fibers, leading to fibrillated failure of the fibers.<sup>56</sup> Apparently, the difference in yarn structure was not found to prominently influence the nature of fiber damage.

## Conclusions

Conventional and modified (compact, SIRO and SIRO-compact) ring-spun yarns were employed to produce dyed woven textiles, which were subjected to simulated repeated laboratory abrasion and laundering to identify the impact of yarn structure on the release of FF mass. All other manufacturing parameters were kept constant for direct comparison. It was found that textiles with modified ring yarn structures released a significantly lower quantity of FF as compared to the textile with the conventional ring yarn. The tensile strength of yarns (removed from the test textiles) was decreased, and breaking elongation increased after repeated abrasion and laundering. However, *t*-tests revealed an insignificant decrease in the tensile strength of SIRO and SIRO-compact yarns, which may be due to the more coherent self-interlocking structure of these yarns. The coefficient of friction was increased for all textile samples after repeated abrasion and laundering; however, the surface roughness showed a decrease for the conventional sample and an increase for the compact, SIRO and SIRO-compact samples after repeated abrasion and laundering. The SEM analysis of the damaged fiber ends identified granulated/transverse and fibrillated damage as the main types of fiber damage. The transverse damage was evident after the first abrasion and laundering cycle and fibrillated damage was prominent after the sixth cycle. The yarn structure did not apparently influence the type of fiber damage. This study reveals that the yarn structure choices impact the number of released FFs, which in turn, are dispersed into the environment as a pollutant, causing potential hazards to the health of the environment and living organisms.

## Declaration of conflicting interests

The author(s) declared no potential conflicts of interest with respect to the research, authorship, and/or publication of this article.

## Funding

The author(s) disclosed receipt of the following financial support for the research, authorship and/or publication of this article: This work was supported by the Engineering and

Physical Sciences Research Council (EPSRC) of UK (grant numbers EP/T024542/1 and EP/T02464X/1).

## ORCID iDs

Alma V Palacios-Marín  <https://orcid.org/0000-0003-0750-786X>

Muhammad Tausif  <https://orcid.org/0000-0003-0179-9013>

## References

1. Athey SN, Adams JK, Erdle LM, et al. The widespread environmental footprint of indigo denim microfibers from blue jeans. *Environ Sci Techn Lett* 2020; 7: 840–847.
2. Zambrano MC, Pawlak JJ, Daystar J, et al. Impact of dyes and finishes on the microfibers released on the laundering of cotton knitted fabrics. *Environ Poll* 2021; 272: 115998.
3. Mishra S, Charan Rath C and Das AP. Marine microfiber pollution: a review on present status and future challenges. *Marin Poll Bullet* 2019; 140: 188–197.
4. Henry B, Laitala K and Klepp IG. Microfibres from apparel and home textiles: prospects for including microplastics in environmental sustainability assessment. *Sci Tot Environ* 2019; 652: 483–494.
5. Acharya S, Rumi SS, Hu Y, et al. Microfibers from synthetic textiles as a major source of microplastics in the environment: a review. *Text Res J* 2021; 91: 2136–2156.
6. Belzagui F, Crespi M, Álvarez A, et al. Microplastics' emissions: microfibers' detachment from textile garments. *Environ Poll* 2019; 248: 1028–1035.
7. Palacios-Marín AV and Tausif M. Fragmented fibre (including microplastic) pollution from textiles. *Text Prog.* 2022; 53: 123–182. DOI: 10.1080/00405167.2022.2066913.
8. Chan CKM, Park C, Chan KM, et al. Microplastic fibre releases from industrial wastewater effluent: a textile wet-processing mill in China. *Environ Chem* 2021; 18: 93–100.
9. De Falco F, Cocca M, Avella M, et al. Microfiber release to water, via laundering, and to air, via everyday use: a comparison between polyester clothing with differing textile parameters. *Environ Sci Techn* 2020; 54: 3288–3296.
10. Cai Y, Mitrano DM, Heuberger M, et al. The origin of microplastic fiber in polyester textiles: the textile production process matters. *J Clean Prod* 2020; 267: 121970.
11. Cesa FS, Turra A, Checon HH, et al. Laundering and textile parameters influence fibers release in household washings. *Environ Poll* 2020; 257: 113553.
12. De Falco F, Di Pace E, Cocca M, et al. The contribution of washing processes of synthetic clothes to microplastic pollution. *Sci Rep* 2019; 9: 1–11.
13. Cai Y, Yang T, Mitrano DM, et al. Systematic study of microplastic fiber release from 12 different polyester textiles during washing. *Environ Sci Techn* 2020; 54: 4847–4855.
14. Sillanpää M and Sainio P. Release of polyester and cotton fibers from textiles in machine washings. *Environ Sci Poll Res* 2017; 24: 19313–19321.

15. Özkan İ and Gündoğdu S. Investigation on the microfiber release under controlled washings from the knitted fabrics produced by recycled and virgin polyester yarns. *J Text Inst* 2021; 112: 264–272.
16. Yang L, Qiao F, Lei K, et al. Microfiber release from different fabrics during washing. *Environ Poll* 2019; 249: 136–143.
17. Kapp KJ and Miller RZ. Electric clothes dryers: an underestimated source of microfiber pollution. *Plos One* 2020; 15: e0239165.
18. O'Brien S, Okoffo ED, O'Brien JW, et al. Airborne emissions of microplastic fibres from domestic laundry dryers. *Sci Tot Environ* 2020; 747: 141175.
19. Kärkkäinen N and Sillanpää M. Quantification of different microplastic fibres discharged from textiles in machine wash and tumble drying. *Environ Sci Poll Res* 2021; 28: 16253–16263.
20. Sun J, Zhu Z-R, Li W-H, et al. Revisiting microplastics in landfill leachate: unnoticed tiny microplastics and their fate in treatment works. *Water Res* 2021; 190: 116784.
21. Zhang Y-Q, Lykaki M, Alrajoula MT, et al. Microplastics from textile origin—emission and reduction measures. *Green Chem* 2021; 23: 5247–5271.
22. Dahlbo H, Aalto K, Eskelinen H, et al. Increasing textile circulation—consequences and requirements. *Sustain Prod Consum* 2017; 9: 44–57.
23. Koszewska M. Circular economy—challenges for the textile and clothing industry. *Aut Res J* 2018; 18: 337–347.
24. Browne MA, Crump P, Niven SJ, et al. Accumulation of microplastic on shorelines worldwide: sources and sinks. *Environ Sci Techn* 2011; 45: 9175–9179.
25. Hernandez E, Nowack B and Mitrano DM. Polyester textiles as a source of microplastics from households: a mechanistic study to understand microfiber release during washing. *Environ Sci Techn* 2017; 51: 7036–7046.
26. Dalla Fontana G, Mossotti R and Montarolo A. Assessment of microplastics release from polyester fabrics: the impact of different washing conditions. *Environ Poll* 2020; 264: 113960.
27. Cai Y, Mitrano DM, Hufenus R, et al. Formation of fiber fragments during abrasion of polyester textiles. *Environ Sci Techn* 2021; 55: 8001–8009.
28. Zambrano MC, Pawlak JJ, Daystar J, et al. Microfibers generated from the laundering of cotton, rayon and polyester based fabrics and their aquatic biodegradation. *Marin Poll Bullet* 2019; 142: 394–407.
29. Zambrano MC, Pawlak JJ, Daystar J, et al. Aerobic biodegradation in freshwater and marine environments of textile microfibers generated in clothes laundering: effects of cellulose and polyester-based microfibers on the microbiome. *Marin Poll Bullet* 2020; 151: 110826.
30. Ladewig SM, Bao S and Chow AT. Natural fibers: a missing link to chemical pollution dispersion in aquatic environments. *Environ Sci Techn* 2015; 49: 12609–12610.
31. Cesa FS, Turra A and Baroque-Ramos J. Synthetic fibers as microplastics in the marine environment: a review from textile perspective with a focus on domestic washings. *Sci Total Environ* 2017; 598: 1116–1129.
32. Periyasamy AP and Tehrani-Bagha A. A review of microplastic emission from textile materials and its reduction techniques. *Poly Degrad Stab* 2022; 199: 1–15.
33. Kim S, Cho Y and Park CH. Effect of cotton fabric properties on fiber release and marine biodegradation. *Text Res J* 2022; 92: 2121–2137.
34. Engelhardt AW. Global development of spun and filament yarns. 4 December 2019. (Accessed on 31 August 2021). <https://www.fiberjournal.com/global-development-of-spun-and-filament-yarns/>
35. Engelhardt A. The fiber year 2009/10: a world survey on textile and nonwovens industry. 2010. (Accessed date: 31 August 2021). [https://www.oerlikon.com/ecomaXL/get\\_blob.php?name=The\\_Fibre\\_Year\\_2010\\_en\\_0607.pdf](https://www.oerlikon.com/ecomaXL/get_blob.php?name=The_Fibre_Year_2010_en_0607.pdf)
36. Hunter L. Cotton spinning technology. In: Gordon S and Hsieh YL (eds) *Cotton science and technology*. Woodhead Publishing, Cambridge, England 2007, pp.240–274.
37. Lawrence CA. *Fundamentals of spun yarn technology*. 1st ed. CRC Press, Boca Raton, Florida 2003.
38. Lawrence CA. *Advances in yarn spinning technology*. Woodhead Publishing, Cambridge England 2010.
39. McNally JP and McCord FA. Cotton quality study: V: resistance to abrasion. *Text Res J* 1960; 30: 715–751.
40. Raja Balasaraswathi S and Rathinamoorthy R. Effect of fabric properties on microfiber shedding from synthetic textiles. *J Text Inst* 2021; 113: 789–809.
41. Palacios-Marín AV, Jabbar A and Tausif M. Fragmented fiber pollution from common textile materials and structures during laundry. *Text Res J*. MirafTAB M (ed). 2022. DOI: 10.1177/00405175221090971.
42. Berruzo M, Bonet-Aracil M, Montava I, et al. Preliminary study of weave pattern influence on microplastics from fabric laundering. *Text Res J* 2021; 91: 1037–1045.
43. Bresee RR, Annis PA and Warnock MM. Comparing actual fabric wear with laboratory abrasion and laundering. *Text Chem Color* 1994; 26: 17–23.
44. Militky J and Ibrahim S. Effect of textile processing on fatigue. In: MirafTAB M (ed) *Fatigue failure of textile fibres*. Woodhead Publishing, Cambridge England 2009, pp.133–168.
45. Soltani P, Vadood M and Johari MSJF. Modeling spun yarns migratory properties using artificial neural network. *Fib Polym* 2012; 13: 1190–1195.
46. Tyagi G. Yarn structure and properties from different spinning techniques. In: Lawrence CA (ed) *Advances in yarn spinning technology*. Woodhead Publishing, Cambridge England 2010, pp.119–154.
47. Soltani P and Johari M. A study on siro-, solo-, compact-, and conventional ring-spun yarns. Part I: structural and migratory properties of the yarns. *J Text Inst* 2012; 103: 622–628.
48. Buharali G and Omeroglu S. Comparative study on carded cotton yarn properties produced by the conventional ring and new modified ring spinning system. *Fib Text East Eur* 2019; 27: 45–51.
49. Soltani P and Johari M. A study on siro-, solo-, compact-, and conventional ring-spun yarns. Part II: yarn strength with relation to physical and structural properties of yarns. *J Text Inst* 2012; 103: 921–930.

50. Gupta B. Friction behavior of fibrous materials used in textiles. In: Gupta B (ed) *Friction in textile materials*. Woodhead Publishing, Cambridge England 2008, pp.67-94.
51. Masen MA. A systems based experimental approach to tactile friction. *J Mech Behav Biomed Mater* 2011; 4: 1620-1626.
52. Hearle JW, Lomas B and Cooke WD. *Atlas of fibre fracture and damage to textiles*. 2nd ed. Woodhead Publishing Ltd, Cambridge England 1998.
53. Pinlova B, Hufenus R and Nowack B. Systematic study of the presence of microplastic fibers during polyester yarn production. *J Clean Prod* 2022; 363: 132247.
54. Yuksekkay ME. More about fibre friction and its measurements. *Text Prog* 2009; 41: 141-193.
55. El Gaiar M and Cusick G. A study of the morphology of cotton-fibre fracture in abrasion tests in relation to the coefficient of friction between the fabric tested and the abradant. *J Text Inst* 1976; 67: 141-145.
56. Textor T, Derksen L, Bahners T, et al. Abrasion resistance of textiles: Gaining insight into the damaging mechanisms of different test procedures. *J Eng Fib Fab* 2019; 14: 1-7.